Seebeck coefficient in polycrystalline $La_{0.7}Sr_{0.3-x}Ag_xMnO_3$ pellets: analysis in terms of a phase separation model

2006 J. Phys.: Condens. Matter 18 493

(http://iopscience.iop.org/0953-8984/18/2/011)

INSTITUTE OF PHYSICS PUBLISHING JOURNAL OF PHYSICS: CONDENSED MATTER

J. Phys.: Condens. Matter **18** (2006) 493–505 doi:10.1088/0953-8984/18/2/011

Seebeck coefficient in polycrystalline $La_{0.7}Sr_{0.3-x}Ag_xMnO_3$ pellets: analysis in terms of a phase separation model

Manjusha Battabyal and T K Dey[1]

Thermo-physical Measurements Laboratory, Cryogenic Engineering Centre, Indian Institute of Technology, Kharagpur 721302, India

E-mail: tapasdey@hijli.iitkgp.ernet.in

Received 14 June 2005, in final form 10 November 2005
Published 14 December 2005
Online at stacks.iop.org/JPhysCM/18/493

Abstract

The temperature dependent resistivity and thermoelectric power of monovalent (Ag) doped $La_{0.7}Sr_{0.3-x}Ag_xMnO_3$ polycrystalline pellets ($x = 0.05, 0.10, 0.20, 0.25$) between 20 and 450 K are reported. Ag substitution enhances the conductivity of this system. The Curie temperature (T_C) also increases from 303 to 364 K with increasing Ag content. In the paramagnetic region ($T > T_C$), the electrical resistivity is well represented by adiabatic polaron hopping, while in the ferromagnetic region ($T < T_C$), the resistivity data show a nearly perfect fit for all the samples to an expression containing the residual resistivity, a two-magnon scattering term and a term associated with small-polaron metallic conduction, which involves a relaxation time due to a soft optical phonon mode. The small-polaron hopping mechanism is found to fit well to the thermoelectric power data for $T > T_C$ and in the high temperature limit for the thermoelectric power is primarily defined by the spin contribution. At low temperatures ($T < T_C$) in the ferromagnetic region, the Seebeck coefficient (S) is well explained with an expression of the type: $S_{FM} = S_0 + S_{3/2}T^{3/2} + S_4T^4$, and confirms the dominant role of electron–magnon scattering. Both resistivity and thermopower data over the entire temperature range are further examined in the light of a two-phase model based on an effective medium approximation. Thermopower data on $La_{0.7}Sr_{0.3-x}Ag_xMnO_3$, computed using measured resistivity and the expression derived using the effective medium approach, give a fairly good description of the observed thermal variation of thermoelectric power in monovalent (Ag) doped $La_{0.7}Sr_{0.3-x}Ag_xMnO_3$.

1. Introduction

Perovskite-like lanthanum manganites display both strong ferromagnetism and metallic conductivity when trivalent La^{3+} ions are partially substituted for divalent ions Ca, Ba, Sr

[1] Author to whom any correspondence should be addressed.

etc [1–5]. Substitution of divalent ions for La^{3+} creates a Mn^{3+}–Mn^{4+} mixed valence state resulting in mobile charge carriers and canting of Mn spins. The double exchange (DE) interaction [6] of Mn^{3+} and Mn^{4+} pairs, along with the Jahn–Teller effect, leads to the appearance of the so-called colossal magneto-resistance (CMR) in such systems. Millis *et al* [7, 8] argued that the physics of manganites is dominated by the interplay between a strong electron–phonon coupling and the large Hund coupling effect that optimizes the electronic kinetic energy by the formation of ferromagnetic phase. However, other factors, namely, average size of the cations, mismatch effects, vacancies in La and Mn sites and the oxygen stoichiometry, also play an important role. Compounds synthesized by partial substitution of lanthanum by monovalent alkali metals such as K^+, Rb^+, Na^+ were reported long ago [9]. Since the valence state of the alkali metal ions is +1, substitution of these ions affects the ratio of Mn^{3+} ($t_{2g}^3e_g^1$) and Mn^{4+} ($t_{2g}^3e_g^0$) ions, which ultimately also influences the DE mechanism. Further, substitution of monovalent ions (K^+, Rb^+, Na^+, Ag^+) for La in $LaMnO_3$ results in increased magneto-resistance [10] and a large magneto-caloric effect [11].

The electrical and magnetic properties of divalent substituted La perovskites have been studied in much detail, compared to those for monovalent substituted systems [10, 12–18]. In general, polaronic transport dominates the electrical conductivity in the paramagnetic region ($T > T_c$), and various electron scattering processes determine the resistivity at low temperatures in the ferromagnetic region ($T < T_c$). It may be mentioned that the very nature of charge carriers in the low temperature metallic state of doped manganites has not yet been settled unambiguously. In a theory of CMR for ferromagnetic manganites, Alexandrov and Bratkovsky [19] proposed that small polaronic transport is the prevalent conduction mechanism even below the ferromagnetic ordering temperature (T_C). Some of the recent experimental studies [20–22] also concluded in favour of polaronic transport in the ferromagnetic metallic state of manganites [21]. Amongst the various transport properties, thermoelectric power (TEP) offers a simple but a sensitive tool to study the scattering mechanisms that dominates the electronic conduction and also provides insight into changes of the band structure near the metal–insulator transition. The Seebeck coefficient has also been subject of several studies [14, 23–31], particularly in divalent-doped manganites. In the high temperature ($T > T_C$) region, most of the reports suggest small-polaron hopping, while below T_C in the ferromagnetic region the TEP is governed by the coexistence of both phonon drag and magnon drag effects.

In the present communication, we report our results on the temperature dependence of the electrical resistivity and TEP of fine-grained samples from the novel manganite series $La_{0.7}Sr_{0.3-x}Ag_xMnO_3$, in which Sr^{2+} ions have been partially replaced by Ag^+ ions; the samples were synthesized by a soft chemical process (pyrophoric method). To our knowledge, detailed studies on the TEP on $La_{0.7}Sr_{0.3-x}Ag_xMnO_3$ compounds have not been reported yet. There exist only a few reports on the electrical properties of lanthanum strontium manganites, in which Ca^{2+}/Sr^{2+} has been partially replaced by K^+/Na^+ [14, 32–36]. Our measured data on the electrical resistivity and thermoelectric power of $La_{0.7}Sr_{0.3-x}Ag_xMnO_3$ compounds, both in the paramagnetic ($T > T_C$) and ferromagnetic phase ($T < T_C$), are discussed in the light of various theoretical propositions. We further confirm that the temperature dependence of the TEP of the $La_{0.7}Sr_{0.3-x}Ag_xMnO_3$ series could be explained fairly well by a two-phase model derived by an effective medium approximation [26].

2. Experimental details

Powder samples of $La_{0.7}Sr_{0.3-x}Ag_xMnO_3$ ($x = 0.05, 0.10, 0.20, 0.25$) with nanometric grains were prepared by a pyrophoric method [37]. The preparation starts from an aqueous,

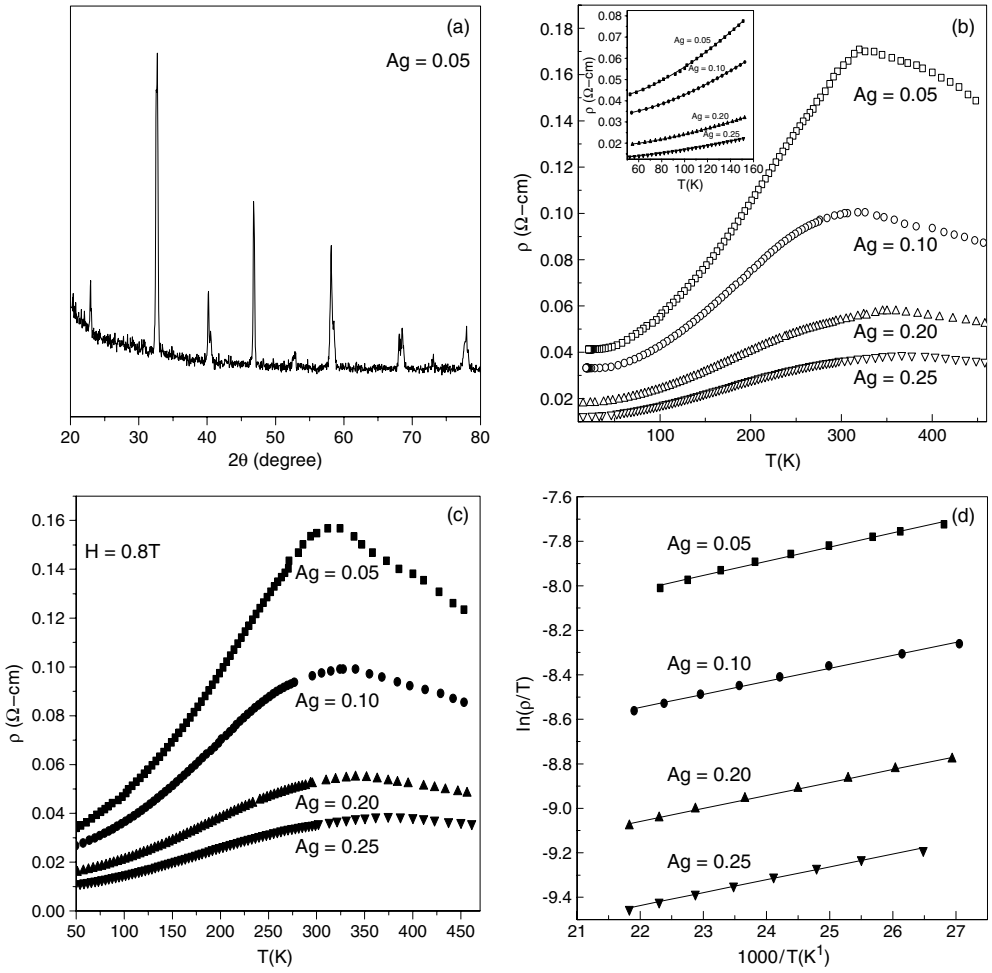

Figure 1. (a) Typical x-ray diffraction pattern for $La_{0.7}Sr_{0.3-x}Ag_xMnO_3$ ($x = 0.05$) pellets. (b) and (c) show the temperature dependence of the electrical resistivity of $La_{0.7}Sr_{0.3-x}Ag_xMnO_3$ ($x = 0.05, 0.10, 0.20, 0.25$) polycrystalline pellets between 10 and 450 K for $H = 0$ and 0.8 T, respectively. The inset in (a) shows the best fit (solid lines) to the experimental data in the ferromagnetic region (150 K $< T <$ 50 K) obtained with equation (11). (d) Shows the plot of $\ln \rho/T$ versus $1000/T$, confirming the small-polaron hopping conduction for $T > T_C$ ($\chi^2 \sim 10^{-7}$).

polymeric-bond precursor solution starting with water-soluble coordinated complexes of the composing metal ions. La_2O_3, $Sr(NO_3)_2$, $AgNO_3$ and $Mn(CH_3COO)_2$ tetra-hydrate (99% purity) have been used as starting materials. The fluffy charred mass obtained after the pyrophoric reaction was crushed and calcined at 800 °C for 8 h. The calcined powders were palletized and sintered at 1000 °C in air for 24 h. The pellets were then slowly furnace cooled to room temperature. XRD of the samples confirmed the single-phase nature of the samples up to the studied composition. A typical XRD pattern of a prepared pellet (Ag = 0.05) is shown in figure 1(a). All the peaks have been indexed in the rhombohedral system with space group $R\bar{3}C$. The calculated lattice parameters are listed in table 1. The crystallite size of the samples is between 30 and 40 nm, as estimated by Debye–Scherer method. Substitution of divalent Sr atoms by monovalent Ag atoms leads to an increase of Mn^{4+} content from 35%

Table 1. Structural and some physical parameters of $La_{0.7}Sr_{0.3-x}Ag_xMnO_3$ compounds.

Sample (x)	$a = b$ (AU)	Mn^{4+} (%)	Oxygen content	Crystallite size (nm)	T_{MI} (K)	T_c (K)	$\rho_{300\ K}$ (Ω cm)	MR_{peak} (%)	MR_{300} (%)
0.05	5.5014	35	3.031	33	319.6	303.6	0.164	1.25	1.93
0.10	5.5036	40	3.026	34	326.1	333.9	0.100	2.52	2.47
0.20	5.5054	50	3.022	37	345.4	354.9	0.054	4.09	2.97
0.25	5.5097	55	3.018	39	366.3	363.4	0.036	16.72	8.76

($x = 0.05$) to 55% ($x = 0.25$). The oxygen content in the studied pellets was also estimated using iodometric redox titration, and the result is given in table 1.

The Currie temperature was determined from the temperature dependence of the AC susceptibility. The temperature dependence of electrical resistivity (ρ) of the pellets, cut into rectangular shape (10 mm × 3 mm × 2 mm), was measured in a cryo refrigerator (APD 202), placed inside the pole gap of an electromagnet. The DC four-probe method, employing a programmable current source (Advantest TR6142) and digital nanovoltmeter (Keithley 181), was adopted to measure the sample resistance. The whole experiment was conducted under computer control. The TEP was measured on the same samples by a differential method. A small heater was used to create a small temperature gradient, which was measured by a calibrated differential Au + 0.07% Fe/Chromel thermocouple. All voltages were measured by a digital nanovoltmeter with a resolution of $\pm 0.01\ \mu V$. The estimated uncertainty in both resistivity and thermopower measurements was within ∼0.5%. Measured TEP data were corrected for the thermopower of the copper leads.

3. Results and discussions

Figures 1(b) and (c) show for $H = 0$ and 0.8 T respectively the resistivity (ρ) as a function of temperature for $La_{0.7}Sr_{0.3-x}Ag_xMnO_3$ ($x = 0.05, 0.10, 0.20, 0.25$) between 10 and 450 K. All the samples show a metallic behaviour at low temperatures and with increasing temperatures undergo a sharp metal–insulator transition at T_{MI}. The highest magneto-resistance observed at 300 K is ∼8.76% for the sample with Ag = 0.25. The increase in electrical conductivity of $La_{0.7}Sr_{0.3-x}Ag_xMnO_3$ with Ag substitution is likely to be associated with the increase in the ratio Mn^{4+}/Mn^{3+}, which causes enhancement of holes in e_g band [14]. The cation valency distribution can be represented as $La^{3+}_{1-x}Sr^{2+}_{x-y}Ag_y(Mn^{3+}_{1-(x+y)}Mn^{4+}_{x+y})O_3$. This shows that the increase of Ag ion by amount y will result in an $(x + y)$ amount increase in Mn^{4+}. Consequently, a small amount of Ag addition results in a large number of charge carriers and the resistivity decreases very significantly. Under the external magnetic field ($H = 0.8$ T), the T_{MI} peak shifts slightly to lower temperatures. The Curie temperature (T_c) increases for low Ag doping and displays a relatively slow rise for higher Ag concentration (table 1). In the low doping region, the Mn^{4+}/Mn^{3+} ratio is favourable to ferromagnetism. However, as the doping level increases, the Mn^{4+} concentration exceeds that of Mn^{3+}, thereby Mn^{3+}–O–Mn^{4+} pairs become fewer. This favours Mn^{4+}–O–Mn^{4+} super-exchange interaction and weakens the DE interaction. This causes the change in transition temperature to be smaller for samples with higher Ag content. Similar observations are reported in $La_{1-x}Ca_{x-y}K_yMnO_3$ [35] as well as sodium doped lanthanum manganites [14].

Figure 2(a) shows the temperature dependence of the absolute TEP measured for the same set of $La_{0.7}Sr_{0.3-x}Ag_xMnO_3$ samples between 50 and 450 K. The magnitude of the absolute TEP decreases with increase in Ag content in the sample, and all the samples show a change-over in the sign of Seebeck coefficient at around T_C, it being positive for $T < T_C$. It may

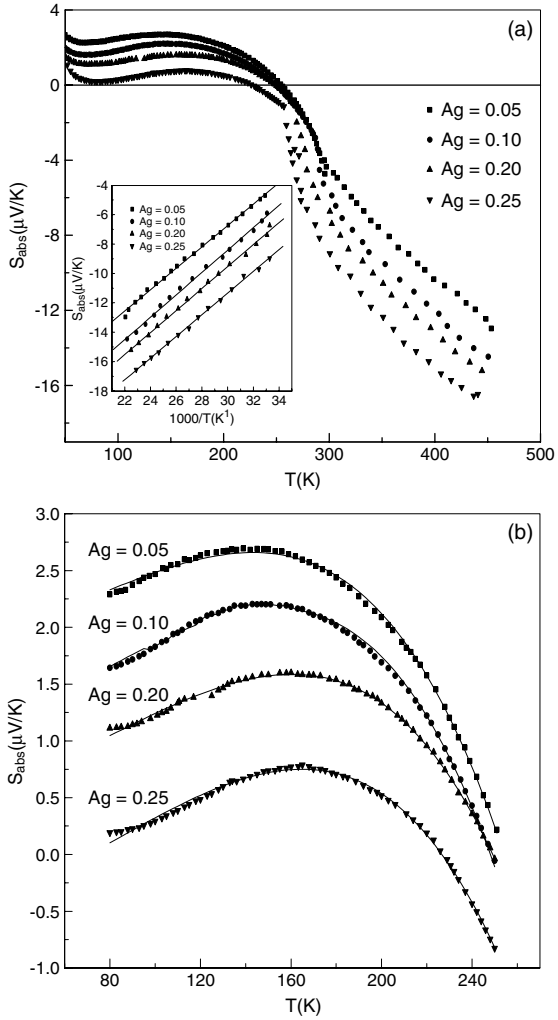

Figure 2. (a) Temperature dependence of absolute thermoelectric power of the same $La_{0.7}Sr_{0.3-x}Ag_xMnO_3$ pellets at zero field between 80 and 450 K. The inset shows an S versus T^{-1} plot for $T > T_C$ according to (2). (b) Temperature dependence of S_{abs} of $La_{0.7}Sr_{0.3-x}Ag_xMnO_3$ pellets in the ferromagnetic region ($T < T_C$). The symbols represent the experimental data and the line represents the best fit to $S_{FM} = S_0 + S_{3/2}T^{3/2} + S_4T^4$.

be noted that the qualitative nature of the thermal variation of TEP is more or less similar to those reported for divalent/monovalent doped $LaMnO_3$. In the low temperature ferromagnetic region, the TEP slowly increases with increasing temperature. It then passes through a broad maximum and decreases rapidly above ∼240 K. The temperature at which the TEP shows the broad maximum shifts to higher temperature with increasing dopant concentration. In the paramagnetic region ($T > T_C$), the TEP is negative and increases monotonically with temperature.

3.1. Resistivity and thermoelectric power ($T > T_C$)

Above the metal–insulator transition temperature (T_{MI}), the Jahn–Teller-type distortion present in the unit cell traps the charge carriers and gives rise to polarons. Many recent

Table 2. Parameters obtained corresponding to the best fit to the experimental data of $La_{0.7}Sr_{0.3-x}Ag_xMnO_3$ pellets between 50 and 450 K.

(x)	ρ_0 (Ω cm)	C (10^{-13}) (Ω cm K$^{-4.5}$)	D (Ω cm)	$\hbar\omega/k_B$ (K)	B (10^{-5} Ω cm K^{-1})	E_p (meV)	$n \times 10^{-19}$ (cm^3)	T_C^{mod} (K)	U_0/k_B (K)
0.05	0.0397	2.919	0.0103	83	7.754	57.71	3.61	335.9	2515
0.10	0.0325	2.863	0.0086	81	5.380	53.47	5.21	338.0	2431
0.20	0.018	1.994	0.0069	79	3.225	50.15	8.69	350.2	2343
0.25	0.012	1.193	0.0043	78	2.236	40.69	12.53	366.3	2208

experiments [13, 29–33] have provided compelling evidence for the existence of polaronic charge carriers in the paramagnetic state of manganites. In the present case, the temperature variation of resistivity in the paramagnetic region between T_{MI} and 450 K follows the adiabatic small-polaron model [38, 39], namely

$$\rho_{PM} = BT e^{E_P/kT}. \tag{1}$$

The corresponding best-fit plot ($\ln \rho/T$ versus $1000/T$) and the best-fit parameters are given in figure 1(d) and table 2 respectively. The carrier concentration (n) is estimated from the parameter B, and as expected, it increases with increasing Ag concentration in $La_{0.7}Sr_{0.3-x}Ag_xMnO_3$.

At high temperature in the paramagnetic insulating (PMI) region, extensive studies have been made on the polaronic transport [40, 41]. The TEP data for $La_{0.7}Sr_{0.3-x}Ag_xMnO_3$ samples for $T > T_C$ (up to ~450 K) fits very well (inset in figure 2(a)) with Mott's equation [42].

$$S_{PM} = \frac{K_B}{e}\left[\frac{E_S}{K_B T} + \alpha'\right] \tag{2}$$

where E_S is the polaron activation energy related to the TEP, and α' is a constant related to the kinetic energy ($=K_B T\alpha'$) of the polarons (carriers). For $\alpha' < 1$, small-polaron hopping conduction occurs, while for $\alpha' > 2$, conduction involves large polarons [43]. The value of α' estimated from equation (2) indicated $\alpha' < 1$, and this confirms the validity of the small-polaron hopping conduction in the temperature dependence of the TEP in the paramagnetic region in this system. It may be mentioned here that although there is no ambiguity regarding a polaronic transport mechanism ($S \propto T^{-1}$) governing the TEP in manganites for $T > T_C$, there exist other views regarding the origin and significance of the temperature independent term of equation (2). Palstra *et al* [44] and Kobayashi *et al* [45] pointed out that the temperature independent term, ($\frac{K_B\alpha'}{|e|} = S_\infty$), is the Seebeck coefficient at the high temperature limit and is a measure of the entropy carried by the mobile particles. Following the extended Heike's generalized expression, S_∞ is expressed as the sum of the conventional configurational term and the term representing the change in spin degeneracy as [44]:

$$S_\infty = \frac{K_B}{|e|}\left[\ln\frac{p}{1-p} + \ln\frac{4}{5}\right]. \tag{3}$$

This expression assumes positively charged mobile carriers, with spin 3/2 in a rigid $S = 2$ system, where p is the fractional hole concentration. Palstra *et al* [44] and Kobayashi *et al* [45] showed for their $La_{1-x}Ca_xMnO_3$ samples that the configurational entropic contribution to the TEP is very small over the entire compositional range $0.1 \leqslant x \leqslant 0.6$. Consequently, S_∞ essentially signifies the spin degeneracy contribution to the thermoelectric power. Palstra *et al* [44] and Kobayashi *et al* [45] evaluated S_∞ ($=-K_B \ln(5/4)/|e|$) for $La_{1-x}Ca_xMnO_3$ ($x = 0.5$) to be -20 μV K^{-1}, which was in good agreement with their measured value (-25 μV). For our $La_{0.7}Sr_{0.3-x}Ag_xMnO_3$ samples ($x = 0.05, 0.10, 0.20, 0.25$) an average

Table 3. Best-fit parameters of the TEP data of $La_{0.7}Sr_{0.3-x}Ag_xMnO_3$.

x	S_0 (μV K^{-1})	$S_{3/2} \times 10^4$ (μV K$^{-5/2}$)	$S_4 \times 10^9$ (μV K^{-5})	E_S (meV)	W_H (meV)	α'
0.05	1.609	9.7	−1.352	8.461	49.25	−0.35
0.10	0.748	12	−1.446	8.027	45.44	−0.36
0.20	0.447	9	−1.032	7.693	42.46	−0.38
0.25	−0.568	10	−1.075	7.256	33.43	−0.39

value of S_∞ (=−28 μV K^{-1}) is obtained from equation (3), which compares very well with −31 μV K^{-1} calculated from the experimental data. This shows that the spin degeneracy contribution constitutes the major component of S_∞, the high temperature limit of the thermoelectric power of $La_{0.7}Sr_{0.3-x}Ag_xMnO_3$ compounds, and thereby supports the above proposition [44, 45].

The polaron activation energy calculated from both resistivity and TEP data (E_P and E_S respectively) is noted in tables 2 and 3. Both E_P and E_S decrease with increase in dopant concentration (x). However, the magnitude of E_S is about one order smaller than E_P. The difference observed arises due to the thermally activated nature of the hopping transport at high temperatures and is a measure of polaron hopping energy $W_H = (E_P - E_S)$. The activation energy (E_P) can be expressed as $E_P = W_H + W_D/2$ for $T > \theta_D/2$ and $E_P = W_D$ for $T < \theta_D/2$, where W_D is the disorder energy. All these parameters of E_P, E_S and W_H are found to decrease with increasing Ag content and are consistent with the observed increase of charge carrier concentration (n). This increased number of charge carriers in the e_g-band participates in conduction, and results in the reduction of the energy needed to release a charge carrier. All these indicate that partial replacement of Sr^{2+} by monovalent Ag^+ causes charge delocalization in the system and consequently a reduction in the polaron-hopping energy (W_H). The nature of the hopping conduction can be further confirmed knowing that the polaron band width J should satisfy the inequality $J > \lambda$ (for adiabatic conditions) and $J < \lambda$ (for nonadiabatic conditions), where λ is given by

$$\lambda = (2K_B T W_H/\pi)^{1/4}(h\upsilon_{ph}/\pi). \tag{4}$$

The estimated values of λ for Ag doped LSMO samples are given in table 4. The polaron bandwidth (J) is calculated from the equation derived by Mott *et al* [42], namely,

$$J \sim e^3[N(E_F)/\varepsilon^3]^{1/2}. \tag{5}$$

Knowing the polaron hopping energy (W_H) and the polaron radius (r_p) [$=\frac{1}{2}(\pi/6N)^{1/3}$], the high frequency dielectric constant of the sample (ε) is calculated from $W_H = (e^2/4\varepsilon)\cdot(r_p^{-1} - R^{-1})$. The density of states at the Fermi level, $N(E_F)$, is obtained by fitting the conductivity data between T_{MI} and $\theta_D/2$ to the variable range hopping (VRH) model, $\sigma = \sigma_0 e^{(-T_0/T)^{1/4}}$, where T_0 is a constant $=16\alpha^3/K_B N(E_F)$. It may be noted that the inequality $J > \lambda$ (table 4) is very well satisfied for all the $La_{0.7}Sr_{0.3-x}Ag_xMnO_3$ samples, confirming the adiabatic hopping nature of the conduction. Finally, the polaron binding energy (W_P) and the polaron mobility (μ_P) are estimated from

$$W_H = \frac{W_P}{2} - J \tag{6}$$

and

$$\mu_P = (\upsilon_{ph} e R^2/KT)\cdot\exp(-W_H/KT). \tag{7}$$

Table 4. Some of the important estimated parameters of $La_{0.7}Sr_{0.3-x}Ag_xMnO_3$ pellets.

(x)	θ_D (K)	$\upsilon_{ph} \times 10^{-13}$ (Hz)	R (AU)	r_P (AU)	$m_P \times 10^{25}$ (g)	$N(E_F) \times 10^{-21}$ (eV^{-1} cm^{-3})	μ_P (cm^2 V^{-1} S^{-1})	γ	J (meV)	λ (meV)	W_P (meV)
0.05	621.8	1.292	4.825	1.945	0.295	2.868	0.067	1.846	43.02	22.88	198.54
0.10	664.8	1.381	4.817	1.943	0.229	3.012	0.072	1.593	41.47	22.84	173.83
0.20	681.6	1.416	4.782	1.931	0.222	3.249	0.075	1.452	40.52	22.17	165.94
0.25	720.6	1.538	4.764	1.925	0.163	3.343	0.078	1.053	37.14	22.13	141.15

The decrease in polaron binding energy (W_P) and increase in polaron mobility (μ_P) (table 4) with increasing Ag content is also in conformity with the observed conductivity displayed by the $La_{0.7}Sr_{0.3-x}Ag_xMnO_3$ system.

3.2. Resistivity and thermoelectric power ($T < T_C$)

Although the resistivity in the low temperature metallic ferromagnetic region well below T_C has been studied by several authors [46–49], the electrical transport mechanism has not yet been resolved unambiguously. Generally, a dominant T^2 contribution is universally observed, which is usually ascribed to electron–electron scattering. Jamie *et al* [46] proposed the origin of the T^2 contribution as being due to single magnon scattering with a cut off at long wavelengths. Zhao *et al* [47], however, questioned the validity of such a mechanism in manganites. Kubo *et al* [49] suggested $\rho_{FM}(T)$ below T_c as:

$$\rho_{FM} = \rho_0 + \rho_2 T^2 + \rho_{4.5} T^{4.5}. \tag{8}$$

Equation (8) predicts the experimental data fairly well. In the equation above, ρ_0 represents the resistivity due to the temperature independent scattering processes, the $\rho_2 T^2$ term corresponds to the electron–electron scattering processes [4, 48], and the $\rho_{4.5} T^{4.5}$ term includes a contribution from the electron–magnon scattering, or spin wave scattering [5, 48]. Recently, Alexandrov *et al* [19] proposed that small-polaronic transport is also a likely mechanism of conduction even below T_C, and the resistivity at low temperatures is given as [50]

$$\rho(T) = \left(\frac{\hbar^2}{ne^2a^2t_p}\right)\frac{1}{\tau}, \tag{9}$$

where t_p, n, a are the effective hopping integral of polarons, carrier density and lattice constant, respectively. The relaxation rate $(1/\tau)$ is

$$\frac{1}{\tau} = \sum_{\alpha} \frac{A_\alpha}{\sinh^2\left(\frac{\hbar\omega_\alpha}{2k_BT}\right)}. \tag{10}$$

In equation (10), ω_α is the average frequency of any optical phonon mode and A_α is a constant, which depends on the electron–phonon coupling length. Due to the factor $1/\sinh^2(\hbar\omega_\alpha/2k_BT)$, only low-lying optical modes (softest ones) with a strong electron–phonon coupling contribute to the low temperature resistivity below T_C. Zhao *et al* [47] included the two-magnon and the impurity scattering to the low temperature resistivity, namely,

$$\rho_{FM}(T) = \rho_0 + \rho_{4.5} T^{4.5} + D/\sinh^2(\hbar\omega_s/2k_BT). \tag{11}$$

The resistivity of $La_{0.7}Sr_{0.3-x}Ag_xMnO_3$ pellets calculated using expression (11) between 50 and ~150 K shows a nearly perfect fit ($\chi^2 \sim < 10^{-8}$) with the measured data (inset in figure 1(b)). The best-fit parameters for the present set of samples are given in table 2. The

fitting parameter ($\hbar\omega_s/k_B$) obtained agrees with that from other reports [47]. The excellent agreement between the measured data and those obtained from equation (11) strongly supports the presence of small polarons and their metallic conduction in the ferromagnetic state at low temperatures as proposed by Alexandrov *et al* [19]. In addition, reports of the isotope effects on the low temperature kinetic and thermodynamic properties also provide clear evidence for a polaronic Fermi liquid state in doped ferromagnetic manganites [20, 21]. Therefore, further analysis of our data was done using equation (11).

As mentioned earlier, in the ferromagnetic regime ($T < T_{MI}$), the TEP of $La_{0.7}Sr_{0.3-x}Ag_xMnO_3$ compounds shows a broad maximum and decreases rapidly at high temperatures. Unlike resistivity, there is no standard relation to interpret the temperature dependence of the TEP in the ferromagnetic phase. Different factors such as impurity, band structure, electron–magnon scattering, electron–phonon scattering, electron–electron correlation, and electron localization, affect the thermal variation of the TEP in many cases. Mandal [27] emphasized the role of electron–magnon scattering and suggested that the magnon drag effect being approximately proportional to the magnon specific heat, one can expect a $T^{3/2}$ contribution in the TEP at low temperature for the FM phase. We, therefore, attempted to analyse the TEP data ($T < T_{MI}$) with an equation of the type [27]

$$S_{FM} = S_0 + S_{3/2}T^{3/2} + S_4T^4 \tag{12}$$

where S_0 is the limiting value of S_{FM} (at $T = 0$ K) and has no physical origin. The $T^{3/2}$ term contributes towards electron–magnon scattering and strongly affects the TEP at low temperatures, while the spin wave fluctuations contribute the S_4T^4 term [5]. The TEP data in the ferromagnetic phase of $La_{0.7}Sr_{0.3-x}Ag_xMnO_3$ compounds agrees well with equation (12) and is shown in figure 2(b). The corresponding best-fit parameters are noted in table 3. Strong influence of electron–magnon scattering at low temperatures ($S_{3/2} \gg S_4$) is clearly evident.

3.3. Application of phase separation model

Thermal variations of the resistivity/TEP of CMR perovskites have been proposed by many authors in terms of phase separation models [26, 40, 51–54]. In the case of doped manganites, Monte Carlo simulation of the double-exchange model with Jahn–Teller coupling also suggested the phase segregation of ferromagnetic metal from antiferromagnetic insulating regimes. As the CMR effect in doped manganites is proved to be larger involving both double exchange and strong coupling to local lattice deformation, the polaronic distortion of the paramagnetic state is thought to persist over some temperature range in the ferromagnetic phase. A number of different experiments [55–57] provide strong evidence for the mixed nature of the transition in the CMR regime. Convincing evidence of two-phase co-existence is found in the Raman data reported by Yoon *et al* [57]. Two contributions in the Raman intensity—a diffusive component associated with small polarons and a continuum contribution from free carriers—have been observed [57]. Jaime *et al* [26, 40] proposed a model using an 'effective medium approach'. The total resistivity of the doped manganite perovskites was then supposed to be due to both band electrons and polarons assuming it to be a two-component system. Accordingly, the conductivity in the metallic regime and the activated conductivity in the polaronic regime are assumed to persist into a mixed phase regime near the metal–insulator transition. In other words, the conductivity in the transition region is supposed to arise due to the mixing factor $C(H, T)$ of the metallic region, embedded in a semiconductive polaronic background, i.e. the conductivity is affected by both polaronic and band electron fractions. Under such circumstances, the effective resistivity $\rho(H, T)$ should satisfy the general expression for ellipsoidal metallic regions of resistivity $\rho_{FM}(T)$ and the

semiconducting region of resistivity $\rho_{PM}(T)$ as [26, 40]

$$\frac{C(\rho-\rho_{FM})}{3}\left(\frac{1}{\rho_{FM}+g_{\parallel}(\rho-\rho_{FM})}+\frac{2}{\rho_{FM}+g_{\perp}(\rho-\rho_{FM})}\right)+\frac{3(1-C)(\rho-\rho_{PM})}{2\rho_{PM}+\rho}=0 \quad (13)$$

where, $g_{\perp} \cong \frac{1}{2}$, $g_{\parallel} = (\frac{b^2\rho_{PM}}{a^2\rho})\ln(1+\frac{a\rho}{b\rho_{PM}})$, with a, b as the major and minor axes of the ellipsoids. From equation (13), one gets

$$C = \frac{1}{1-\frac{(\rho-\rho_{FM})(\rho+2\rho_{PM})\Delta}{9(\rho-\rho_{PM})}} \quad (14)$$

where

$$\Delta = \frac{1}{\rho_{FM}+g_{\parallel}(\rho-\rho_{FM})}+\frac{2}{\rho_{FM}+\frac{(\rho-\rho_{FM})}{2}}. \quad (15)$$

Equation (14) shows that metallic concentration varies with temperature due to the competition between the contributions of the high temperature resistivity (ρ_{PM}) and that due to low temperature resistivity (ρ_{FM}). Incorporating the appropriate expressions for ρ_{PM} (equation (1)) and ρ_{FM} (equation (11)), the metallic concentration $C(H, T)$ is computed between 50 K $< T <$ 450 K and taking $a/b = 25$ ($H = 0$ for all the cases). Figure 3(a) shows the concentration of metallic regions $C(H, T)$ extracted from the resistivity data. From figure 3(a), it is reasonable to expect T_C to equal to the temperature for which $C(H, T)$ equals 0.5. It may be noted that T_C of the studied samples (corresponding to $C = 0.5$ in figure 3(a)) is within ~7% of the measured value. However, the exact shape of $C(H, T)$ curves depends on the form of the effective medium model chosen (a/b) and becomes sharper for lower percolation threshold. It also depends on the nature of the temperature variation of the resistivity around the transition temperature. In order to show the validity of this effective medium approach in transport properties of manganites, Jaime *et al* [26] modified the expression for the Seebeck coefficient $S(H, T)$ proposed by Bergman *et al* [58]. Considering that the effective conductivities match the high and low temperature values in their respective limits, the TEP expression was derived as

$$S(H,T) = \frac{(S_{FM}-S_{PM})(\kappa_{lt}-\kappa_{ht})}{(\kappa_{ht}\rho_{PM}-\kappa_{lt}\rho_{FM})}\frac{\rho_{FM}\rho_{PM}}{(\rho_{PM}-\rho_{FM})} + \frac{(S_{FM}\rho_{PM}-S_{PM}\rho_{FM})}{(\rho_{PM}-\rho_{FM})}+\frac{(S_{PM}-S_{FM})\kappa(H,T)\rho(H,T)}{(\kappa_{ht}\rho_{PM}-\kappa_{lt}\rho_{FM})}. \quad (16)$$

The electronic contribution to the thermal conductivity of lanthanum manganites being only a minor fraction, equation (16) is further simplified as

$$S(H,T) = \frac{[\rho_{PM}S_{FM}-\rho_{FM}S_{PM}+\rho(H,T)(S_{PM}-S_{FM})]}{(\rho_{PM}-\rho_{FM})} \quad (17)$$

where S_{FM} and S_{PM} are the low and high temperature part of the TEP data, respectively.

Using the above expressions for ρ_{PM}, ρ_{FM}, S_{PM} and S_{FM}, $S(T)$ is calculated from equation (17) between 50 and 450 K and is plotted in figure 3(b). It is seen that a fairly good agreement with the experimental data for all the samples could be achieved over an extended temperature range from 80 to 450 K without using any adjustable parameter. As discussed by Jaime *et al* [26], this simple mean-field model ignores many features, which should be included in a complete treatment. Nevertheless, the simplified phenomenological approach based on the effective medium approximation provides an excellent description of the transport properties of $La_{0.7}Sr_{0.3-x}Ag_xMnO_3$ compounds and lends a strong support to the coexistence of metallic regions within a semiconductive polaronic matrix having an activated conductivity.

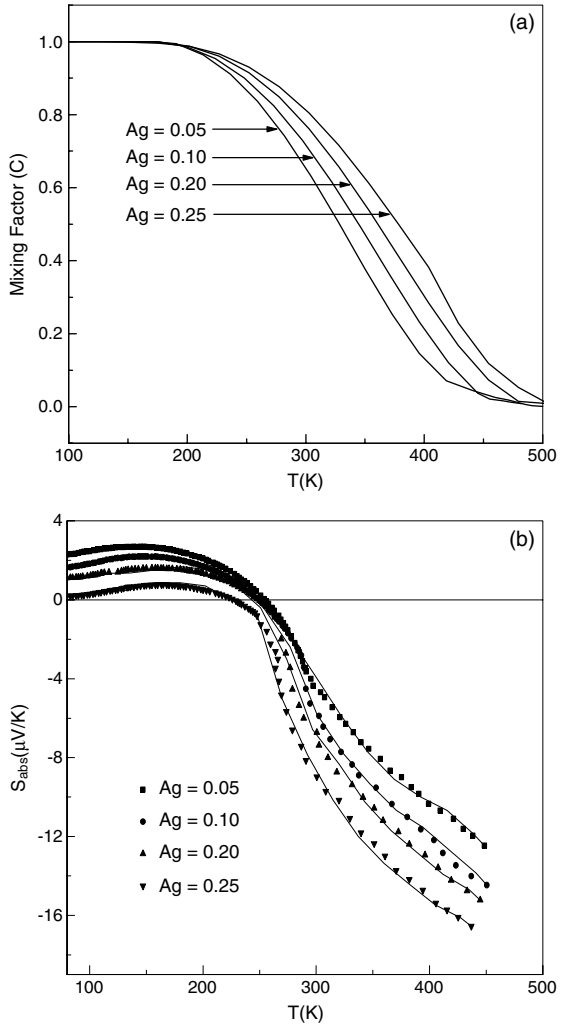

Figure 3. Two-phase analysis of resistivity and thermoelectric power. (a) The concentration of metallic regions $C(H, T)$ extracted from the resistivity data of $La_{0.7}Sr_{0.3-x}Ag_xMnO_3$ (x = 0.05, 0.10, 0.20, 0.25) using the effective medium approach and assuming elongated conducting regions with the ratio $a/b = 25$ for zero field. (b) Solid lines are the values computed using the effective medium approximation (equation (17)). Symbols are the measured data.

4. Conclusions

The electrical resistivity and thermoelectric power between 10 and 450 K of $La_{0.7}Sr_{0.3-x}Ag_xMnO_3$ polycrystalline pellets prepared by a pyrophoric technique are reported. All samples show a sharp metal–insulator transition, and the conductivity of the system enhances with increase in Ag doping. The Curie temperature (T_C) is enhanced from 303.6 to 363.4 K with Ag substitution. For $T > T_C$, the electrical transport is by usual small-polaron hopping. At low temperatures in the ferromagnetic state, the resistivity data give an excellent fit to $\rho_{FM}(T) = \rho_0 + \rho_{4.5}T^{4.5} + D/\sinh^2(\hbar\omega_s/2k_BT)$, which takes into account the role of small polarons and the two-magnon contribution. The temperature variation of the

thermoelectric power in the ferromagnetic region ($T < T_C$) agrees well with an expression of the type $S_{FM} = S_0 + S_{3/2}T^{3/2} + S_4T^4$, and signifies a dominant role of electron–magnon scattering. A simple two-component phenomenological model based on an effective medium approximation has been used to calculate the concentration of the metallic region $C(H = 0, T)$ from the measured resistivity data. Our analysis confirms that the temperature dependence of the thermoelectric power of $La_{0.7}Sr_{0.3-x}Ag_xMnO_3$ pellets computed using measured resistivity and the expression derived using the effective medium approach provides a fairly good description of the measured data in lanthanum manganites of the type $La_{0.7}Sr_{0.3-x}Ag_xMnO_3$.

Acknowledgments

The authors are grateful to Professor S K Ghatak for many helpful discussions. Financial support received from the Department of Science and Technology (New Delhi) in the form of a research project is also gratefully acknowledged.

References

[1] Rao C N R and Raychaudhuri A K 1988 *Colossal Magneto Resistance, Charge Ordering and Related Properties of Manganese Oxides* ed C N R Rao and B Raveau (Singapore: World Scientific) p 1
[2] Ramirez A P 1997 *J. Phys.: Condens. Matter* **9** 8171
[3] Salamon M B and Jaime M 2001 *Rev. Mod. Phys.* **73** 583
[4] Coey J M D, Viret M, Ranno L and Ounadjela K 1995 *Phys. Rev. Lett.* **75** 3910
[5] Urushibara A, Moritomo Y, Arima T, Asamitsu A, Kido G and Tokura Y 1995 *Phys. Rev.* B **51** 14103
[6] Zener C 1951 *Phys. Rev.* **81** 440
[7] Millis A J, Littlewood P B and Shraiman B L 1995 *Phys. Rev. Lett.* **74** 5144
[8] Millis A J 1996 *Phys. Rev.* B **53** 8434
[9] Voorhoeve R J H, Remeika J P, Trimble L F, Cooper A S, Disalvo F J and Gallagher P K 1975 *J. Solid State Chem.* **14** 395
[10] Tao T, Cao Q Q, Gu K M, Xu H Y, Zhang S Y and Du Y W 2000 *Appl. Phys. Lett.* **77** 723
[11] Tang T, Gu K M, Cao Q Q, Wang D H, Zhang S Y and Du Y W 2000 *J. Magn. Magn. Mater.* **222** 110
[12] Pi L, Hervieu M, Maignan A, Martin C and Raveau B 2003 *Solid State Commun.* **126** 229
[13] Abdelmoula N, Cheikh-Rouhou A and Reversat L 2001 *J. Phys.: Condens. Matter* **13** 449
[14] Roy S, Guo Y Q, Venkatesh S and Ali N 2001 *J. Phys.: Condens. Matter* **13** 9547
[15] Wang Z M, Tang T, Wan Y P, Zhang S Y and Du Y W 2002 *J. Magn. Magn. Mater.* **246** 254
[16] Ye S L, Song W H, Dai J M, Wang K Y, Wang S G, Zhang C L, Du J J, Sun Y P and Fang J 2002 *J. Magn. Magn. Mater.* **248** 26
[17] Wang X L, Kennedy S J, Liu H K and Dou S X 1998 *J. Appl. Phys.* **83** 7177
[18] Rao G H, Sun J R, Barner K and Hamad N 1999 *J. Phys.: Condens. Matter* **11** 1523
[19] Alexandrov A S and Bratkovsky A M 1999 *Phys. Rev. Lett.* **82** 141
[20] Zhao G, Wang Y S, Kang D J, Prellier W, Rajeswari M, Keller H, Venkatesan T, Chu C W and Greene R L 2000 *Phys. Rev.* B **62** R11949
[21] Alexandrov A S, Zhao G, Keller H, Lorenz B, Wang Y S and Chu C W 2001 *Phys. Rev.* B **64** 140404
[22] Nucara A, Perucchi A, Calvani P, Aselage T and Emin D 2003 *Phys. Rev.* B **68** 174432
[23] Asamitsu A, Moritomo Y and Tokura Y 1996 *Phys. Rev.* B **53** R2952
[24] Hundley M F and Neumeir J J 1997 *Phys. Rev.* B **55** 11511
[25] Uhlenbruck S, Buchner B, Cross R, Freimuth A, de Guevara A M L and Revcolevschi A 1998 *Phys. Rev.* B **57** R5571
[26] Jaime M, Ln P, Chun S, Salamon M, Dorsey P and Rubinstein M 1999 *Phys. Rev.* B **60** 1028
[27] Mandal P 2000 *Phys. Rev.* B **61** 14675
[28] Sun Y, Xu X and Zhang Y 2000 *Phys. Rev.* B **63** 054404
[29] Banerjee A, Pal S, Bhattacharya S, Chaudhuri B K and Yang H D 2001 *Phys. Rev.* B **64** 104428
[30] Bhattacharya S, Banerjee A, Pal S, Mukherjee R K and Chaudhuri B K 2003 *J. Appl. Phys.* **93** 356
[31] Horyn R, Zaleski A J, Sulkowski C, Bukowska E and Sikora A 2003 *Physica* C **387** 280

[32] Ng-Lee Y, Safina F, Martinez E, Folgado J V, Ibanez R, Beltran D, Lloret F and Segura A 1997 *J. Mater. Chem.* **7** 1905
[33] Sahana M, Singh R N, Shivakumara C, Vasanthacharya N Y, Hegde M S, Subramanium S, Prasad V and Subramanyam S V 1997 *Appl. Phys. Lett.* **70** 2909
[34] Abdelmoula N, Dhahri E, Fourati N and Reversat L 2004 *J. Alloys Compounds* **365** 25
[35] Bhattacharya S, Pal S, Mukherjee R K, Chaudhuri B K and Neeleshwar S 2004 *J. Magn. Magn. Mater.* **269** 359
[36] Zemni S, Dhahri Ja, Cherif K, Dhahri J, Oumezzine M, Ghedira M and Vincent H 2005 *J. Alloys Compounds* **392** 55
[37] Ray A and Dey T K 2003 *J. Magn. Magn. Mater.* **266** 268
[38] Holstein T 1959 *Ann. Phys.* **8** 343
[39] Worledge D C, Jeffrey Snyder G, Beasley M R, Geballe T H, Hiskes R and DiCarolis S 1996 *J. Appl. Phys.* **80** 5158
[40] Jaime M, Salamon M B, Pettit K, Rubenstein M, Treece R E, Horwitz J S and Chrisey D B 1996 *Appl. Phys. Lett.* **68** 1576
Chatterjee S, Chou P H, Chang C F, Hong I P and Yang H D 2000 *Phys. Rev.* B **61** 6106
[41] Jaime M, Salamon M B, Rubenstein M, Treece R E, Horwitz J S and Chrisey D B 1996 *Phys. Rev.* B **54** 11914
[42] Mott N F and Davis E A 1971 *Electronics Processes in Non Crystalline Materials* (Oxford: Clarendon)
[43] Austin I G and Mott N F 1969 *Adv. Phys.* **18** 41
[44] Palstra T T M, Ramirez A P, Cheong S W, Zegarski B R, Schiffer P and Zaanen J 1997 *Phys. Rev.* B **56** 5104
[45] Kobayashi W, Terasaki I, Mikami M, Funahashi R, Nomura T and Katsufuji T 2004 *J. Appl. Phys.* **95** 6825
[46] Jaime M, Lin P, Salamon M B and Han P D 1998 *Phys. Rev.* B **58** R5901
[47] Zhao G, Smolyaninova V, Prellier W and Keller H 2000 *Phys. Rev. Lett.* **84** 6086
Zhao G, Keller H and Prellier W 2000 *J. Phys.: Condens. Matter* **12** L361
[48] Jeffrey Snyder G, Hikes R, DiCarolis S, Beasley M R and Geballe T H 1996 *Phys. Rev.* B **53** 14434
[49] Kubo K and Ohata N 1972 *J. Phys. Soc. Japan* **33** 21
[50] Lang I G and Firsov Yu A 1963 *Sov. Phys.—JEPT* **16** 1301
[51] Bastiaansen P J M and Knops H J F 1998 *J. Phys. Chem. Solids* **59** 297
[52] Li G, Zhou H D, Feng S J, Fan X J, Li X G and Wang Z D 2002 *J. Appl. Phys.* **92** 1406
[53] Kim K H, Uehara M, Hess C, Sharma P A and Cheong S W 2000 *Phys. Rev. Lett.* **84** 2961
[54] de Andres A, Garcia-Hermandez M and Martinez J L 1999 *Phys. Rev.* B **60** 7328
[55] Louca D and Egami T 1999 *Phys. Rev.* B **59** 6193
Billinge S J L, Di Francesco P G, Kwei G H, Neumeier J J and Thompson J D 1996 *Phys. Rev. Lett.* **77** 715
[56] Dai A J P, Fernandez-Baca N, Wakabayashi N, Plummer E W, Tomioka Y and Tokura Y 2000 *Phys. Rev. Lett.* **85** 2553
[57] Yoon S, Liu H, Schollere G, Cooper S, Han P, Payne D, Cheong S and Fisk Z 1998 *Phys. Rev.* B **58** 2795
[58] Bergman D and Stroud D 1990 *Solid State Physics* vol 46, ed H Ehrenreich and D Turnbull (New York: Academic) p 147